

Short-range charge order in $R\text{NiO}_3$ perovskites ($R=\text{Pr, Nd, Eu, Y}$) probed by x-ray-absorption spectroscopy

Cynthia Piamonteze,^{1,2} Hélio C. N. Tolentino,¹ Aline Y. Ramos,^{1,3} Nestor E. Massa,⁴ Jose A. Alonso,⁵ Maria J. Martínez-Lope,⁵ and Maria T. Casais⁵

¹Laboratório Nacional Luz Síncrotron, Caixa Postal 6192, 13084-971 Campinas/SP, Brazil

²IFGW/UNICAMP, 13083-970 Campinas/SP, Brazil

³LMCP-UMR, 7590 CNRS, Paris, France

⁴LANAIS, CEQUINOR, UNLP, C.C. 962, 1900 La Plata, Argentina

⁵Instituto de Ciencia de Materiales de Madrid, C.S.I.C., Cantoblanco, E-28049 Madrid, Spain

(Received 10 August 2004; published 25 January 2005)

The short-range organization around Ni atoms in orthorhombic $R\text{NiO}_3$ ($R=\text{Pr, Nd, Eu}$) perovskites has been studied over a wide temperature range by Ni K -edge x-ray-absorption spectroscopy. Our results demonstrate that two different Ni sites, with different average Ni-O bond lengths, coexist in those orthorhombic compounds and that important modifications in the Ni nearest-neighbors environment take place across the metal-insulator transition. We report evidences for the existence of short-range charge order in the insulating state, as found in the monoclinic compounds. Moreover, our results suggest that the two different Ni sites coexist even in the metallic state. The coexistence of two different Ni sites, independently on the R ion, provides a common ground to describe these compounds and sheds interesting light in the understanding of the phonon-assisted conduction mechanism and unusual antiferromagnetism present in all $R\text{NiO}_3$ compounds.

DOI: 10.1103/PhysRevB.71.012104

PACS number(s): 71.30.+h, 63.20.-e, 75.30.Mb, 78.70.Dm

Lanthanide nickel perovskites ($R\text{NiO}_3$, $R=\text{lanthanide}$) display, except for $R=\text{La}$, a thermally driven first-order metal-insulator (MI) transition¹⁻³ and an unusual antiferromagnetic order.⁴⁻⁶ The detailed atomic and electronic structures, and their modifications at the crossover from localized to itinerant electronic behavior, remain among the most important questions to be addressed. The crossover temperature (T_{MI}) to the metallic state increases as the lanthanide ion decreases, showing a close relation between T_{MI} and the structural distortion. These $R\text{NiO}_3$ compounds are at the boundary between low- Δ metals and charge-transfer insulators.^{7,8} The charge-transfer energy Δ is smaller than the $3d$ - $3d$ Coulomb repulsion, so that the band gap is controlled by $\sim\Delta - W$, where W is the one-electron bandwidth. Ni^{3+} in low-spin configuration ($t_{2g}^6 e_g^1$) is a Jahn-Teller (JT) ion with a single e_g electron with orbital degeneracy. Owing to strong hybridization among the $\text{Ni}3d:e_g$ and $\text{O}2p:\sigma$ bands, some holes are transferred from the $3d$ to the $2p$ orbitals in the ground state, leading to partial screening of the JT distortion.

The long-range structure of the lighter lanthanide ($R=\text{Pr, Nd, Sm, Eu}$) compounds is orthorhombic ($Pbnm$ space group), with rather regular NiO_6 octahedra, in both metallic and insulating states.² Upon decreasing the temperature through the transition, a sudden slight increase in the average Ni-O bond length ($\Delta_{\text{Ni-O}}=0.004$ Å), followed by the steric accommodation in the tilts of the octahedra ($\Delta\phi=-0.5^\circ$) was reported.² It was proposed³ that the closing of the gap stems from the increase of the bandwidth W , which depends on the Ni-O-Ni bond angle ($180^\circ-\phi$) through $W \propto \cos \phi$. This description is incomplete since, in the metallic state, infrared studies point to a conduction mediated by strong electron-phonon coupling associated to local charge fluctuations.⁹ The significant shift observed in T_{MI} by ^{16}O - ^{18}O isotope substitution¹⁰ is an additional indication of a

JT-polaron assisted conduction mechanism. Furthermore, our recent reports on the decreased hybridization of the Ni-O bonding⁸ and on the splitting in the coordination shell,¹¹ in the insulating state, emphasize that local modifications within the NiO_6 octahedra play a fundamental role in the understanding of the MI transition.

In the insulating state of the heavier lanthanide ($R=\text{Ho, Y, Er, Tm, Yb, Lu}$) compounds, the long-range structure is monoclinic ($P2_1/n$ space group).^{6,12} The $P2_1/n$ symmetry implies the existence of small Ni^I and large Ni^{II} sites. Alonso *et al.* associated this monoclinic distortion to a long-range charge order along the three axes. The small site (Ni^I) has stronger hybridization among $\text{Ni}3d$ and $\text{O}2p$ orbitals than the large one (Ni^{II}). Moreover, the large site (Ni^{II}) presents a larger JT distortion, with a more localized single e_g electron. Zhou and Goodenough¹³ suggested that the difference in charge transfer between the $3d$ and $2p$ orbitals in each Ni site would give rise to the charge order. The existence of charge-ordered Ni sites establishes a favorable scenario to understand the unusual magnetic structure that requires alternating couplings.⁴⁻⁶ Alonso *et al.* found different magnetic moments for each Ni site: 0.7 and $1.4\mu_B$ for the small and large Ni sites in YNiO_3 , respectively.⁶

Concerning lighter lanthanide compounds, attempts to observe long-range charge order by neutron diffraction have been unsuccessful.^{4,5,10} Recently, electron diffraction and Raman scattering¹⁴ and resonant x-ray scattering¹⁵ studies produced evidences on a small monoclinic distortion in NdNiO_3 thin films. Even if the extension of these results to polycrystalline compounds is not straightforward, they question the validity of the assignment of the orthorhombic symmetry and single magnetic moment associated to Ni in the lighter lanthanide compounds. More recently, evidences that the low-temperature distortion is shared by all members of the $R\text{NiO}_3$ family have been presented.¹⁶

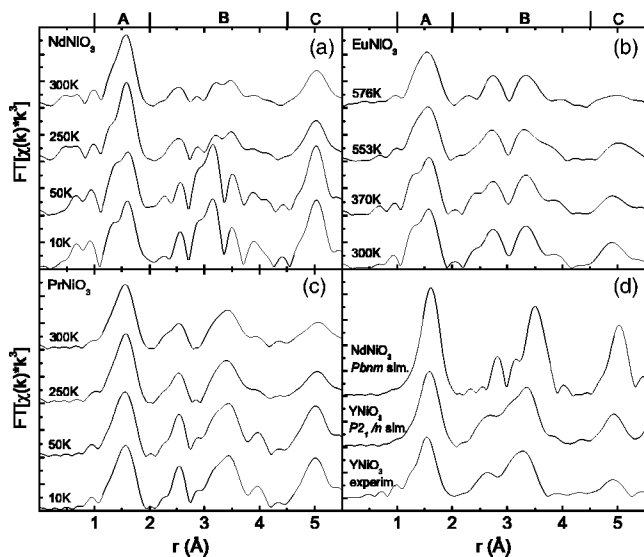


FIG. 1. Fourier transform of Ni K -edge EXAFS signal for (a) NdNiO_3 , (b) EuNiO_3 , (c) PrNiO_3 at selected temperatures and for (d) YNiO_3 at room temperature. Simulations for $P2_1/n$ and $Pbnm$ space groups also shown in (d).

We report on an EXAFS (extended x-ray-absorption fine structure) spectroscopy study on the lighter lanthanide ($R=\text{Pr, Nd, Eu}$) compounds. We present evidences of the coexistence of two different Ni sites in these orthorhombic compounds, over a wide temperature range, providing a common background to describe the whole $R\text{NiO}_3$ family. The polycrystalline samples studied were described elsewhere.¹⁷ EXAFS measurements were carried out at the XAS beam line of LCLS, Brazil,¹⁸ using a Si(111) monochromator, with an energy resolution of 2.4 eV at Ni K -edge. Spectra were measured in transmission mode up to a maximum wave number of $k \approx 19 \text{ \AA}^{-1}$. A cryostat heater was used to control the temperature from 10 to 600 K.

Figure 1 shows the Fourier transform (FT) amplitude of the experimental EXAFS signal for NdNiO_3 ($T_{MI}=200 \text{ K}$), EuNiO_3 ($T_{MI}=460 \text{ K}$), and PrNiO_3 ($T_{MI}=130 \text{ K}$) at a few selected temperatures, with two spectra in the metallic and two in the insulating states. The FT represents a pseudoradial distribution function around Ni atoms, where the r values are shifted by a small amount due to the phase shift of the photoelectron wave function.¹⁹ A clear splitting, associated to the existence of separable bond lengths in the coordination shell (peak A around 1.6 \AA), is observed for both NdNiO_3 and EuNiO_3 in the insulating state [Figs. 1(a) and 1(b)]. The splitting is not well resolved but an asymmetry in the low- r values is observed for PrNiO_3 [Fig. 1(c)]. In the metallic state [Figs. 1(a)–1(c)], peak A is asymmetric for all compounds. We also show the FT amplitude for the monoclinic insulating compound YNiO_3 ($T_{MI}=582 \text{ K}$) and two simulations using FEFF7 (Ref. 19) [Fig. 1(d)]. Peak A for YNiO_3 displays a similar asymmetry. Simulations have been performed based on the crystallographic structure found by neutron diffraction for YNiO_3 (Ref. 6) and NdNiO_3 .² The simulation for YNiO_3 with the $P2_1/n$ space group, which includes the two nonequivalent Ni sites, reproduces very well the overall YNiO_3 spectrum [Fig. 1(d)], with a slight

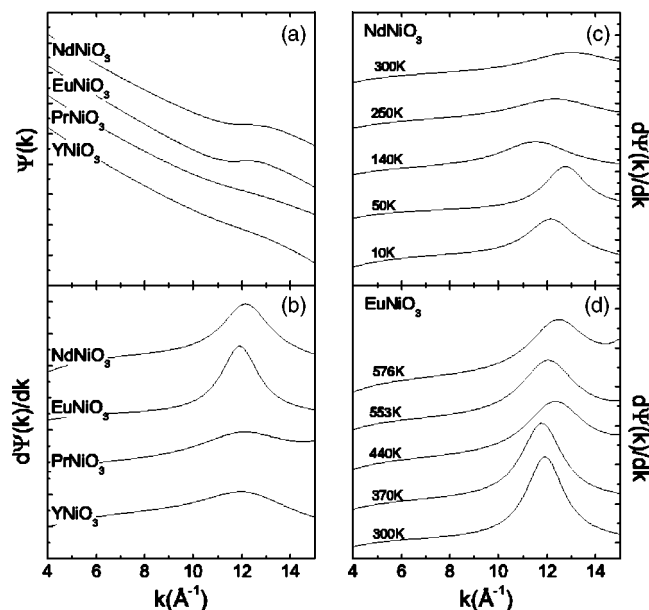


FIG. 2. (a) Phase and (b) phase derivative (PD) functions for $R\text{NiO}_3$ in the insulating state. PD functions for (c) NdNiO_3 and (d) EuNiO_3 across the MI transition.

asymmetry in the coordination shell. On the other hand, the simulation for NdNiO_3 with the $Pbnm$ space group [Fig. 1(d)] produces a sharper coordination shell, with no asymmetry or splitting at all, as expected from a single Ni environment. The comparison of the NdNiO_3 ($Pbnm$) simulation with the experimental low-temperature NdNiO_3 spectrum [Fig. 1(a)] demonstrates that a single Ni site cannot describe the short-range Ni environment. On the other hand, the medium and long-range structure is quite well reproduced with the orthorhombic symmetry, showing that the splitting is really taking place only at the short-range scale.

The EXAFS signal obtained from the combination of two Ni sites, with identical backscattering atoms but with slightly different average bond lengths, presents a beating in the amplitude function.²⁰ The wave number where the beating occurs (k_b) satisfies $\delta r \cdot k_b \approx \pi/2$, where δr is the separation in bond length.^{20,21} This beating in the EXAFS amplitude generates a splitting in the FT amplitude (as seen in peak A, Fig. 1). The phase function $\Psi(k)$, extracted from the peak A analysis by the inverse FT, gives an inflection point that leads to an extremum in the phase derivative (PD) function [Figs. 2(a) and 2(b)]. The PD analysis is a very sensitive tool to follow small separations between two close distances, particularly in distorted perovskites.²² Figure 2(a) shows the phase functions extracted by back-transforming peak A (Fig. 1) taking the average Ni-O bond lengths for the $R\text{NiO}_3$ ($R=\text{Nd, Eu, Pr, Y}$) compounds. Maxima appear around the beating position $k_b \approx 12.3 \text{ \AA}^{-1}$ in the PD function [Fig. 2(b)] and give an unambiguous signature of the existence of the two well separated Ni-O bond lengths. An estimation of the separation value of roughly $\delta r \approx 0.12 \text{ \AA}$ can be deduced from the beating position. This value is affected by systematic errors²¹ and is slightly overestimated. The average separation found for YNiO_3 and for all heavier lanthanide compounds^{6,12} is $\delta r \approx 0.09 \text{ \AA}$. This value can be used to cor-

rect for systematic errors and calibrate the scale. What is important to remark here is that the PD maximum occurs at about the same position for all compounds.

The PD analysis, as well as the FT splitting, supports the coexistence of two Ni sites with different average bond lengths. The lighter lanthanide ($R=\text{Pr, Nd, Eu}$) compounds, as the heavier lanthanide ones, present small and large Ni sites with a similar separation of about $\delta r \approx 0.09 \text{ \AA}$ among them. Owing to the similarity among all $R\text{NiO}_3$ compounds, we conclude that, at the short-range scale probed by EXAFS, a similar charge-order modulation takes place in the insulating state. Nevertheless, only in the heavier lanthanide compounds this charge-order modulation develops at long range and gives rise to the lowering of the crystallographic symmetry from orthorhombic to monoclinic. The behavior of the PD function with increasing temperature for NdNiO_3 and EuNiO_3 [Figs. 2(c) and 2(d)] shows that the amplitude at the inflection point decreases but does not vanish and remains around the same position for $T > T_{MI}$. Above the first-order transition, in the metallic state, conduction electrons moving through the lattice destroy charge order and the amount of split Ni sites diminishes. But, two different Ni bond lengths, with roughly the same separation, are still present. This result suggests that, in the metallic state, regions of split Ni sites survive and coexist immersed in the conducting matrix, in accordance with a recent infrared spectroscopy study.¹⁶ The coexistence of more localized electrons in a Fermi-liquid background have also been suggested to be a common feature in $R\text{NiO}_3$ compounds.^{23,24} These phase inhomogeneities should be delocalized and fluctuating within the material. The conduction mechanism, which is strongly coupled to the lattice,¹⁰ is intimately related to these fluctuations.

The structural crossover can be studied by the Debye-Waller factor $\exp(-2\sigma^2 k^2)$, which damps the EXAFS signal and the FT amplitude. This factor contains static and thermal contributions.¹⁹ The static contribution comes from the bond-length dispersion around the average value. The thermal contribution is related to the lattice vibrations, which decreases with temperature and can be well described by correlated Einstein or Debye models.²⁵ To quantify the modifications observed in the FT amplitude (Fig. 1), we performed an EXAFS analysis limited to $k=12 \text{ \AA}^{-1}$ using theoretical amplitude and phase functions¹⁹ and an average Ni coordination shell. This restricted k range characterizes a low-resolution study in r space, where the Ni-O bond lengths are no longer distinguishable and the bond length separation appears as a static contribution to the total disorder. Figure 3 shows the total disorder of the coordination shell ($\sigma_{\text{Ni-O}}^2$, peak A in Fig. 1) and of the fifth Ni shell (σ_{NiNi}^2 , peak C in Fig. 1) for NdNiO_3 . $\sigma_{\text{Ni-O}}^2$ follows the expected thermal behavior from room temperature down to 170 K, then smoothly increases down to 90 K and remains constant. When the temperature is increased, a structural hysteresis is observed, consistent with the first-order character of the transition, illustrated by the measured resistance with temperature. Subtracting the extrapolated thermal behavior from the total disorder of the coordination shell, one gets the increase in bond length dispersion from the metallic to the insulating state. This experimental increase is about 0.0012 \AA^2 (Fig. 3). This value is related to the amount of split Ni sites changing at the cross-

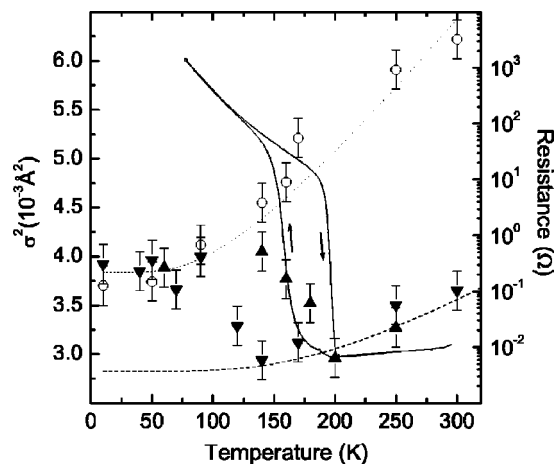


FIG. 3. Total disorder for the NdNiO_3 coordination shell while decreasing (\blacktriangledown) and increasing (\blacktriangle) the temperature, and for Ni shell at 5 \AA (\circ). Thermal behavior for the coordination shell (---) and Ni shell (\cdots), and resistance (—).

over. If one considers the crossover from a “pure metallic” state (one single Ni site with bond length of 1.95 \AA) to a “pure insulating” state (long-range charge-ordered Ni^{I} and Ni^{II} sites with bond length separation of 0.09 \AA) an increase in bond length dispersion of $\Delta\sigma_{\text{Ni-O}}^2 \approx 0.0020 \text{ \AA}^2$ should be found. This is much larger than the experimental value (0.0012 \AA^2), indicating that only a fraction of Ni sites is splitting at the crossover. On the other hand, σ_{NiNi}^2 exhibits the expected smooth thermal decrease with temperature, showing that the splitting in bond length takes place only at the short-range restricted to the coordination shell. Similar behaviors have been obtained for EuNiO_3 and PrNiO_3 .

The local structural modification evidenced by $\sigma_{\text{Ni-O}}^2$ takes place in a broader temperature range (80 K) than that of resistance measurement (25 K). The sharp electronic transition is then related to a smoother local structural modification. Across the first-order MI transition, the system gets into a state where the volume fraction of the localized-electron phase increases but the metallic phase does not disappear abruptly. The coexistence of metallic and nonmetallic phases has already been invoked to explain some peculiarities of the electrical resistivity and Seebeck coefficient in NdNiO_3 .²⁶ In $R\text{NiO}_3$ compounds, we believe that regions of a localized-electron phase exist in the metallic matrix above T_{MI} , but the conduction electrons prevent the charge-order state and the split sites are fluctuating. When the temperature goes below T_{MI} , the electron localization triggers the transition and the volume fraction of these regions grows. The system undergoes a structural phase transition into a long-range charge-ordered state, with $P2_1/n$ symmetry, in the case for the heavier lanthanide compounds.^{6,12} In the case of the lighter lanthanides, the modulation is limited to a short-range scale. The compound remains disordered at long range and there is no breaking in the $Pbnm$ symmetry.² The presence of JT-distorted sites and short-range charge order in the insulating state of the orthorhombic compounds gives an explanation to the strange antiferromagnetic arrangement that requires two nonequivalent Ni sites.^{4,5} As in the monoclinic compounds,

two different magnetic moments can now be associated to Ni. In both orthorhombic and monoclinic compounds, the crossover from the insulating to the metallic state can be regarded as a melting of the charge order but with important local dynamical distortion fluctuations still remaining. The persistence of these fluctuations, associated to local distortion of NiO₆ octahedra, explains the phonon-assisted conduction mechanism in the metallic state, as suggested by Medarde *et al.*¹⁰

In conclusion, we demonstrated by using EXAFS spectroscopy that important modifications take place in the Ni coordination shell of RNiO₃ compounds across the MI transition. Our results give evidences of the coexistence of two different Ni sites and short-range charge order in the insulat-

ing states of polycrystalline RNiO₃ ($R=Pr, Nd, Eu$) orthorhombic compounds, as earlier found in the monoclinic systems. The existence of short-range charge order in these compounds provides a common ground to describe their transport properties and unusual antiferromagnetism. The coexistence of two phases in the metallic state, a fluctuating localized-electron phase with JT-distorted sites immersed in a conducting matrix, sheds interesting light in some intriguing properties, like the phonon-assisted conduction mechanism.

Work was partially supported by LNLS/ABTLuS. C.P. thanks FAPESP for financial support.

-
- ¹P. Lacorre, J. B. Torrance, J. Pannetier, A. I. Nazzal, P. W. Wang, and T. C. Huang, *J. Solid State Chem.* **91**, 225 (1991).
- ²J. L. García-Muñoz, J. Rodríguez-Carvajal, P. Lacorre, and J. B. Torrance, *Phys. Rev. B* **46**, 4414 (1992).
- ³J. B. Torrance, P. Lacorre, A. I. Nazzal, E. J. Ansaldo, and C. Niedermayer, *Phys. Rev. B* **45**, R8209 (1992).
- ⁴J. L. García-Muñoz, J. Rodríguez-Carvajal, and P. Lacorre, *Phys. Rev. B* **50**, 978 (1994).
- ⁵J. Rodríguez-Carvajal, S. Rosenkranz, M. Medarde, P. Lacorre, M. T. Fernández-Díaz, F. Fauth, and V. Trounov, *Phys. Rev. B* **57**, 456 (1998).
- ⁶J. A. Alonso, J. L. García-Muñoz, M. T. Fernández-Díaz, M. A. G. Aranda, M. J. Martínez-Lope, and M. T. Casais, *Phys. Rev. Lett.* **82**, 3871 (1999).
- ⁷T. Mizokawa, A. Fujimori, T. Arima, Y. Tokura, N. Mōri, and J. Akimitsu, *Phys. Rev. B* **52**, 13 865 (1995).
- ⁸C. Piamonteze, H. C. Tolentino, F. C. Vicentin, A. Y. Ramos, N. E. Massa, J. A. Alonso, M. J. Martínez-Lope, and M. T. Casais, *Surf. Rev. Lett.* **9**, 1121 (2002).
- ⁹N. E. Massa, J. A. Alonso, M. J. Martínez-Lope, and I. Rasines, *Phys. Rev. B* **56**, 986 (1997).
- ¹⁰M. Medarde, P. Lacorre, K. Conder, F. Fauth, and A. Furrer, *Phys. Rev. Lett.* **80**, 2397 (1998).
- ¹¹C. Piamonteze, H. C. Tolentino, A. Y. Ramos, N. E. Massa, J. A. Alonso, M. J. Martínez-Lope, and M. T. Casais, *Physica B* **320**, 71 (2002).
- ¹²J. A. Alonso, M. J. Martínez-Lope, M. T. Casais, J. L. García-Muñoz, and M. T. Fernández-Díaz, *Phys. Rev. B* **61**, 1756 (2000).
- ¹³J.-S. Zhou and J. B. Goodenough, *Phys. Rev. B* **69**, 153105 (2004).
- ¹⁴M. Zaghroui, A. Bulou, P. Lacorre, and P. Laffez, *Phys. Rev. B* **64**, 081102(R) (2001).
- ¹⁵U. Staub, G. I. Meijer, F. Fauth, R. Allenspach, J. G. Bednorz, J. Karpinski, S. M. Kazadov, L. Paolasini, and F. d'Acapito, *Phys. Rev. Lett.* **88**, 126402 (2002).
- ¹⁶F. de la Cruz, C. Piamonteze, N. E. Massa, H. Salva, J. A. Alonso, M. J. Martínez-Lope, and M. T. Casais, *Phys. Rev. B* **66**, 153104 (2002).
- ¹⁷J. A. Alonso, M. J. Martínez-Lope, and M. A. Hidalgo, *J. Solid State Chem.* **116**, 146 (1995).
- ¹⁸H. C. N. Tolentino, A. Y. Ramos, M. C. M. Alves, R. A. Barrea, E. Tamura, J. C. Cezar, and N. Watanabe, *J. Synchrotron Radiat.* **8**, 1047 (2001).
- ¹⁹J. J. Rehr and R. C. Albers, *Rev. Mod. Phys.* **72**, 621 (2000).
- ²⁰G. Martens, P. Rabe, N. Schwentner, and A. Werner, *Phys. Rev. Lett.* **39**, 1411 (1977).
- ²¹H. Jaffrès, P. L. Fèvre, H. Magnan, A. Midoir, D. Chandèsris, L. Ressler, A. Schuhl, F. N. V. Dau, M. Goiran, J. P. Peyrade, and A. R. Fert, *Phys. Rev. B* **61**, 14 628 (2000).
- ²²R. A. Souza, N. M. Souza-Neto, A. Y. Ramos, H. C. N. Tolentino, and E. Granado, *Phys. Rev. B* **70**, 214426 (2004).
- ²³J.-S. Zhou, J. B. Goodenough, B. Dabrowski, P. W. Klamut, and Z. Bukowski, *Phys. Rev. B* **61**, 4401 (2000).
- ²⁴J.-S. Zhou, J. B. Goodenough, and B. Dabrowski, *Phys. Rev. B* **67**, 020404(R) (2003).
- ²⁵E. Sevillano, H. Meuth, and J. J. Rehr, *Phys. Rev. B* **20**, 4908 (1979).
- ²⁶X. Granados, J. Fontcuberta, X. Obradors, L. Mañosa, and J. B. Torrance, *Phys. Rev. B* **48**, 11 666 (1993).